Asia Pac. J. Math. 2023 **10**:5

HYBRID CONTROL OF THE HOPF BIFURCATION FOR ADVERTISING CAPITAL MODEL: ANALYTICAL AND NUMERICAL INVESTIGATION

QI WANG*, XUEYANG LIU, JIEYI YAO

School of Mathematics and Statistics, Guangdong University of Technology, Guangzhou, China

*Corresponding author: qiwang@gdut.edu.cn

Received Nov. 29, 2022

Abstract. In this paper, a hybird control Euler method is proposed in which state feedback and parameter perturbation are used to control the Hopf bifurcation of a nonlinear advertising capital model. Firstly, the numerical bifurcation of the original delay differential equation is discussed by using the Hopf bifurcation theory. Secondly, the criterion of the Hopf bifurcation of the controlled system and its discrete scheme at the positive equilibrium point is established as well as the direction of the Hopf bifurcation is studied. Finally, the effectiveness of the control strategy for Hopf bifurcation is verified by numerical experiments.

2020 Mathematics Subject Classification. 65P30; 65L12.

Key words and phrases. Advertising capital model; Euler method; Hopf bifurcation; Hybrid control; Local stability.

1. Introduction

In the last two decades, there has been great interest in dynamical characteristics of delay differential equations (DDEs). Especially, many research has been devoted to the Hopf bifurcation of DDEs. Hopf bifurcation is a common feature of nonlinear DDEs and has become an important aspect in the study of the differential equations. There is a large number of results about stability and Hopf bifurcation of DDEs, the interested readers can refer to the papers [9, 12, 21].

In order to explain the advertising effect with mathematics and apply it in market research better, Luhta and Virtanen [8] built a delay feedback model of the relationship between advertising and goodwill according to the classic Nerlove-Arrow (NA) model [10]. In the literature,

DOI: 10.28924/APJM/10-5

©2023 Asia Pacific Journal of Mathematics

advertising is considered to be influenced by the stock of goodwill, which cumulatively calculates the influence of the company's current and past advertising expenditure. The addition of nonlinear term and time delay in NA dynamic equation makes the model more realistic and more abundant dynamic properties are shown. So we consider the following DDEs to describe the advertising capital model

$$\begin{aligned} &\dot{x}(t) = -ax(t) + bx(t-\tau)e^{-b\left(\frac{x(t-\tau)}{d}\right)^2}, \quad t \geq 0, \\ &x(t) = \phi(x), \quad -\tau \leq t \leq 0, \end{aligned} \tag{1}$$

where $x(t)$ is the stock of goodwill at time t, $bx(t-\tau)e^{-b\left(\frac{x(t-\tau)}{d}\right)^2}$ is the advertising expenditure at time $t-\tau$, a is the depreciation coefficient, a, b, d, τ are positive constants, $\phi(x)$ is a continuous nonnegative function and $\phi \in C([-\tau, 0], \mathbb{R}^+)$, $\phi(0) > 0$.

There are few studies on the dynamic behavior of Eq. (1). Luhta and Virtanen [8] analyzed the stability of the equilibriums numerically and the behavior of chaos for the discrete model of Eq. (1). Gao and Ruan [3] discussed the Hopf bifurcation of Eq. (1) theoretically. Wang et al. [13] studied the analytical and numerical oscillation of Eq. (1) by using the θ-methods. As for the numerical control of Eq. (1), we have not found any results in the literature. In fact, it is important to determine the stability and bifurcation condition of the equilibrium point in some systems [7,14,18]. For an enterprise, if the behavior of goodwill is cyclical or chaotic, it will be difficult to estimate goodwill and formulate advertising strategies [1,4]. So it is meaningful to use numerical method to control its bifurcations. Recently, bifurcation control has attracted a lot of attention and a variety of bifurcation control methods are introduced [5,15,17,22]. The aim of bifurcation control is to delay (advance) the onset of an inherent bifurcation, change the parameter value of an existing bifurcation point, stabilize a bifurcated solution or branch. Such as, in [16], the hybrid control nonstandard finite-difference scheme is used to control the Hopf bifurcation. Different from [16], in this paper, we construct a hybrid control Euler method in which state feedback and parameter perturbation are used to control the Hopf bifurcation of Eq. (1). The results show that the dynamic behavior of a controlled system can be changed by choosing appropriate control parameters. For any step-size, we obtain the consistent dynamical results of the corresponding differential equation.

The remainder of the article is structured as follows. In Section 2, we take the time delay as the bifurcation parameter and some sufficient conditions for the delay induced bifurcation of uncontrolled system are discussed. In Section 3, the hybrid control method is applied to

control the Hopf bifurcation of the controlled system. In Section 4, the stability of the Hopf bifurcation of the controlled system are determined by discussing the distribution of roots of characteristic equation of discrete system. In Section 5, the direction and stability of bifurcating periodic solutions of the controlled system are determined by using the bifurcation theory of discrete systems. In Section 6, some numerical simulations are carried out. In the final section, we summarize our work and and the future was prospected.

2. Numerical Hopf Bifurcation in Uncontrolled System

Let $u(t) = x(\tau t)$, then Eq. (1) can be written as

$$\dot{u}(t) = -a\tau u(t) + b\tau u(t-1)e^{-b(\frac{u(t-1)}{d})^2}. \tag{2}$$

It is easy to see that the positive equilibrium point u_* of Eq. (2) satisfies

$$a = be^{-b(\frac{u_*}{d})^2}. \tag{3}$$

For the function $F(x) = -ax + bxe^{-b(\frac{x}{d})^2}$, we have

$$F'(x) = -a + e^{-\frac{bx^2}{d^2}}\left(b - \frac{2b^2x^2}{d^2}\right), \tag{4}$$

since $F'(0) = b - a > 0$ when $b > a$, so $u_* = d\sqrt{\frac{1}{b}\ln\frac{b}{a}}$ is unique.

Application of Euler method to Eq. (2) gives

$$u_{n+1} = u_n + h\left(-a\tau u_n + b\tau u_{n-m}e^{-b(\frac{u_{n-m}}{d})^2}\right). \tag{5}$$

Set $y_n = u_n - u_*$, then Eq. (5) changes into

$$y_{n+1} = y_n + h\left(-a\tau(y_n + u_*) + b\tau(y_{n-m} + u_*)e^{-b(\frac{y_{n-m}+u_*}{d})^2}\right). \tag{6}$$

Apparently, the origin is an equilibrium point of Eq. (6). Then the linearization of Eq. (6) at the origin gives

$$y_{n+1} = (1 - a\tau h)y_n + a\tau h\left(1 - \frac{2bu_*^2}{d^2}\right)y_{n-m}, \tag{7}$$

whose characteristic equation is

$$\lambda^m(\lambda - 1 + a\tau h) - a\tau h\left(1 - \frac{2bu_*^2}{d^2}\right) = 0. \tag{8}$$

In the following, we analyze the distribution of characteristic root according to Ruan and Wei [11] and Zhang et al. [23].

Lemma 1. [23] *Suppose that $B \in \mathbb{R}$ is a bounded, closed and connected set, $f(\lambda,\tau) = \lambda^m + p_1(\tau)\lambda^{m-1} + p_2(\tau)\lambda^{m-2} + \cdots + p_m(\tau)$ is continuous in $(\lambda,\tau) \in \mathbb{C} \times B$. Then as τ varies, the sum of the order of the zeros of $f(\lambda,\tau)$ out of the unit circle $\{\lambda \in \mathbb{C} : |\lambda| > 1\}$ can change only if a zero appears on or crosses the unit circle.*

Suppose that $e^{i\omega}$ is a root of Eq. (8), then differentiating both sides of Eq. (8) with respect to τ gives

$$\frac{d\lambda}{d\tau} = -\frac{ah(2bu_*^2 - d^2) + ahd^2\lambda^m}{d^2\lambda^m(m+1) + d^2\lambda^{m-1}(ahm\tau - m)}, \tag{9}$$

together with

$$\frac{d|\lambda|^2}{d\tau} = \lambda\frac{d\bar{\lambda}}{d\tau} + \bar{\lambda}\frac{d\lambda}{d\tau} \tag{10}$$

we obtain

$$\frac{d|\lambda|^2}{d\tau}|_{\tau=0,\lambda=1} = -\frac{4ahbu_*^2}{d^2} < 0. \tag{11}$$

Consequently, $|\lambda| < 1$ for sufficiently small $\tau > 0$, so there exists the maximal $\tau^{'} > 0$ such that all roots of Eq. (8) have no modulus of root more than one for $0 < \tau < \tau^{'}$.

In order to find $\tau^{'}$, substitute $e^{i\omega_k}$ into Eq. (8) and separate the real part and imaginary part

$$\begin{cases} \cos\omega_k - a\tau h\left(1 - \frac{2bu_*^2}{d^2}\right)\cos m\omega_k = 1 - a\tau h, \\ \sin\omega_k + a\tau h\left(1 - \frac{2bu_*^2}{d^2}\right)\sin m\omega_k = 0, \end{cases} \tag{12}$$

so we have

$$\cos\omega_k = 1 + \frac{2a^2\tau^2h^2u_*^2b(1 - \frac{bu_*^2}{d^2})}{d^2(1 - a\tau h)} \tag{13}$$

and

$$\tau_k = \frac{\sin\omega_k}{ah(\frac{2bu_*^2}{d^2} - 1)\sin m\omega_k}. \tag{14}$$

To make (13) holds we assume that $bu_*^2 > d^2$. Moreover we get

$$\begin{aligned} d_h &= \frac{dr_k^2(\tau)}{d\tau}|_{\tau=\tau_k,\omega=\omega_k} = \left(\lambda\frac{d\bar{\lambda}}{d\tau} + \bar{\lambda}\frac{d\lambda}{d\tau}\right)|_{\tau=\tau_k,\omega=\omega_k} \\ &= \frac{2(1-\cos\omega_k)(m(2-ah\tau_k)+1)}{\tau_k|ahm\tau - m + (m+1)e^{i\omega_k}|^2}, \end{aligned} \tag{15}$$

so $d_h > 0$ for sufficiently small $h > 0$.

From the above analysis, we can obtain the following theorem for Eq. (5).

Theorem 1. *(i) If $bu_*^2 < d^2$, then the equilibrium point u_* of Eq. (5) is asymptotically stable for any $\tau \geq 0$.*

(ii) If $bu_*^2 > d^2$, then the equilibrium point u_* is asymptotically stable for $\tau \in [0, \tau')$, and unstable for $\tau > \tau'$, Eq. (5) undergoes a Hopf bifurcation at u_* when $\tau = \tau'$.

3. Hopf Bifurcation in Hybrid Control System

Similar to [2,6,16,20], the hybrid control method are implemented to Eq. (2). The controlled advertising capital model is constructed as follows

$$\dot{u}(t) = \alpha\left(-a\tau u(t) + b\tau u(t-1)e^{-b(\frac{u(t-1)}{d})^2}\right) + (1-\alpha)\tau\left(u(t-1) - u_*\right), \tag{16}$$

where $0 < \alpha \leq 1$.

It is not difficult to compute that Eq. (16) and Eq. (2) share the same positive equilibrium point u_*.

Set $z(t) = u(t) - u_*$, Eq. (16) becomes

$$\dot{z}(t) = \alpha\left(-a\tau(z(t)+u_*) + b\tau(z(t-1)+u_*)e^{-b(\frac{(z(t-1)+u_*)}{d})^2}\right) + (1-\alpha)\tau z(t-1). \tag{17}$$

Linearize Eq. (17) at $z = 0$ gives

$$\dot{z}(t) = \alpha a\tau\left(\left(1 - \frac{2u_*^2 b}{d^2}\right)z(t-1) - z(t)\right) + (1-\alpha)\tau z(t-1), \tag{18}$$

whose characteristic equation is

$$\lambda = \alpha a\tau\left(\left(1 - \frac{2u_*^2 b}{d^2}\right)e^{-\lambda} - 1\right) + (1-\alpha)\tau e^{-\lambda}. \tag{19}$$

From Eq. (19) we know that $\lambda < 0$ when

$$\frac{2u_*^2 b}{d^2} > \frac{1-\alpha}{\alpha a}. \tag{20}$$

Further for $\omega \neq 0$, $i\omega$ is a root of Eq. (19) if and only if

$$i\omega = \alpha a\tau\left(\left(1 - \frac{2u_*^2 b}{d^2}\right)e^{-i\omega} - 1\right) + (1-\alpha)\tau e^{-i\omega}. \tag{21}$$

Separating real part and imaginary part from Eq. (21), we get

$$\begin{cases} \left(\alpha a\tau\left(1 - \frac{2u_*^2 b}{d^2}\right) + (1-\alpha)\tau\right)\cos\omega &= \alpha a\tau, \\ \left(\alpha a\tau\left(1 - \frac{2u_*^2 b}{d^2}\right) + (1-\alpha)\tau\right)\sin\omega &= -\omega, \end{cases} \tag{22}$$

so

$$\omega = \pm\tau\sqrt{\left((1-\alpha) - \alpha a\frac{2u_*^2 b}{d^2}\right)\left((1-\alpha) + \alpha a\left(2 - \frac{2u_*^2 b}{d^2}\right)\right)}, \tag{23}$$

it is easy to see that (23) holds under the condition

$$\frac{2u_*^2 b}{d^2} > 2 + \frac{1-\alpha}{\alpha a}. \tag{24}$$

From (22) we compute that

$$\tau_k = \arcsin\left(-\frac{\omega}{\alpha a\tau(1-\frac{2u_*^2 b}{d^2}) + (1-\alpha)\tau}\right) + 2k\pi, k = 0, 1, 2, \cdots. \tag{25}$$

Set

$$\omega_0 = \tau\sqrt{\left((1-\alpha) - \alpha a\frac{2u_*^2 b}{d^2}\right)\left((1-\alpha) + \alpha a\left(2 - \frac{2u_*^2 b}{d^2}\right)\right)}. \tag{26}$$

Let $\lambda_k = \alpha_k(\tau) + i\omega_k(\tau)$ be a root of Eq. (19) near $\tau = \tau_k$ such that $\alpha_k(\tau_k) = 0, \omega_k(\tau_k) = \omega_0$. Then we have the following lemma.

Lemma 2. $\alpha_k^{'}(\tau_k) > 0$.

Proof. Differentiating both sides of Eq. (19) with respect to τ, we get

$$\frac{d\lambda}{d\tau} = \frac{e^{-\lambda}(2a\alpha bu_*^2 + \alpha d^2(1-a) - d^2) + a\alpha d^2}{\tau e^{-\lambda}(2a\alpha bu_*^2 + \alpha d^2(1-a) - d^2) - d^2}, \tag{27}$$

so

$$\frac{d\lambda}{d\tau}|_{\tau=\tau_k} = \frac{(2a\alpha bu_*^2 + \alpha d^2(1-a) - d^2)(\cos\omega_0 - i\sin\omega_0) + a\alpha d^2}{\tau(2a\alpha bu_*^2 + \alpha d^2(1-a) - d^2)(\cos\omega_0 - i\sin\omega_0) - d^2}, \tag{28}$$

which implies that

$$\alpha_k^{'}(\tau_k) = \frac{1}{\Delta}(a\alpha d^2 + \tau_k(2a\alpha bu_*^2 + \alpha d^2(1-a) - d^2)), \tag{29}$$

where

$$\begin{aligned}\Delta = &\left(\tau_k\cos\omega_0(2a\alpha bu_*^2 + \alpha d^2(1-\alpha) - d^2) - d^2\right)^2 \\ &+ \left(\tau_k\sin\omega_0(2a\alpha bu_*^2 + \alpha d^2(1-\alpha) - d^2)\right)^2,\end{aligned}$$

by virtue of (24) and $2a\alpha bu_*^2 + \alpha d^2(1-a) - d^2 > a\alpha d^2 > 0$ we have $\alpha_k^{'}(\tau_k) > 0$. The proof is finished. □

Set

$$\frac{1-\alpha}{\alpha a} < \frac{2u_*^2 b}{d^2} < 2 + \frac{1-\alpha}{\alpha a}. \tag{30}$$

Theorem 2. *For Eq. (16),*

(i) If (30) holds, then $u = u_*$ is asymptotically stable;

(ii) If (24) holds, then $u = u_*$ is asymptotically stable for $\tau \in [0, \tau_0)$, unstable for $\tau > \tau_0$, Eq. (16) undergoes a Hopf bifurcation at u_* when $\tau = \tau_k, k = 0, 1, 2, \cdots$.

4. Stabilization of Euler Hybrid Control System

In this section, we implement the hybrid control strategy to discuss the stability and bifurcation of the numerical discrete control system. Application of Euler method to Eq. (16), we obtain

$$u_{n+1} = (1 - a\alpha\tau h)u_n + h\alpha b\tau u_{n-m} e^{-b(\frac{u_{n-m}}{d})^2} + h\tau(1-\alpha)(u_{n-m} - u_*). \tag{31}$$

Let $v(t) = u(t) - u_*$, then Eq. (31) becomes

$$v_{n+1} = (1 - a\alpha\tau h)v_n + h\alpha b\tau(v_{n-m} + u_*)e^{-b(\frac{v_{n-m}+u_*}{d})^2} + h(1-\alpha)\tau v_{n-m} - a\tau\alpha u_* h. \tag{32}$$

Introducing a new variable $V_n = (v_n, v_{n-1}, \cdots, v_{n-m})^T$, we can rewrite Eq. (32) as

$$V_{n+1} = \tilde{F}(V_n, \tau), \tag{33}$$

where $\tilde{F} = (\tilde{F}_0, \tilde{F}_1, \cdots, \tilde{F}_m)^T$ and

$$\bar{F}_k = \begin{cases} (1-a\alpha\tau h)v_{n-k} + h\alpha b\tau(v_{n-m-k} + u_*)e^{-b(\frac{v_{n-m-k}+u_*}{d})^2} \\ \qquad + h(1-\alpha)\tau v_{n-m-k} - a\tau\alpha u_* h, \ k = 0, \\ v_{n-k+1}, \ 1 \le k \le m. \end{cases} \tag{34}$$

Linearization of Eq. (33) at origin gives

$$V_{n+1} = \tilde{A}V_n, \tag{35}$$

where

$$\tilde{A} = \begin{bmatrix} a_m & 0 & \cdots & 0 & 0 & a_0 \\ 1 & 0 & \cdots & 0 & 0 & 0 \\ 0 & 1 & \cdots & 0 & 0 & 0 \\ \vdots & \vdots & \ddots & \vdots & \vdots & \vdots \\ 0 & 0 & \cdots & 1 & 0 & 0 \\ 0 & 0 & \cdots & 0 & 1 & 0 \end{bmatrix} \tag{36}$$

and

$$a_m = 1 - a\alpha\tau h, a_0 = a\alpha\tau h\left(1 - \frac{2bu_*^2}{d^2}\right) + h(1-\alpha)\tau.$$

Thus, the characteristic equation of $\tilde{A}$ is

$$\lambda^m(\lambda - 1 + a\alpha\tau h) - a\alpha\tau h\left(1 - \frac{2bu_*^2}{d^2}\right) - h(1-\alpha)\tau = 0. \tag{37}$$

Lemma 3. *If (20) holds, then all the roots of Eq. (37) have modulus less than one for sufficiently small* $\tau > 0$.

Proof. When $\tau = 0$, Eq. (37) becomes

$$\lambda^{m+1} - \lambda^m = 0, \tag{38}$$

then Eq. (37) has an m-fold root and a simple root $\lambda = 1$.

Consider the root $\lambda(\tau)$ which is a differentiable function of τ and depends continuously on τ, satisfies $|\lambda(0)| = 1$. From Eq. (37), we obtain

$$\frac{d\lambda}{d\tau} = -\frac{h(\lambda^m a\alpha d^2 + 2a\alpha b u_*^2 - a\alpha d^2 + \alpha d^2 - d^2)}{\lambda^{m-1} d^2 (a\alpha h m\tau + \lambda m - m + \lambda)} \tag{39}$$

and

$$\frac{d\bar{\lambda}}{d\tau} = -\frac{h(\bar{\lambda}^m a\alpha d^2 + 2a\alpha b u_*^2 - a\alpha d^2 + \alpha d^2 - d^2)}{\bar{\lambda}^{m-1} d^2 (a\alpha h m\tau + \bar{\lambda} m - m + \bar{\lambda})}, \tag{40}$$

thus

$$H = \frac{d|\lambda|^2}{d\tau}|_{\tau=0,\lambda=1} = -\frac{h(2a\alpha b u_*^2 + (\alpha - 1)d^2)}{d^2}. \tag{41}$$

It is easy to know that $H < 0$ when (20) holds, so all the roots of Eq. (37) lie in $|\lambda| < 1$ for sufficiently small $\tau > 0$. □

Lemma 4. *If (30) holds, then for any* $\tau > 0$ *and sufficiently small* $h > 0$, *the characteristic equation Eq. (37) has no root on unit circle.*

Proof. Suppose that $e^{i\omega_k}$ is a root of Eq. (37), then

$$e^{i(m+1)\omega_k} - e^{im\omega_k}(1 - a\alpha\tau h) - a\alpha\tau h\left(1 - \frac{2bu_*^2}{d^2}\right) - h(1-\alpha)\tau = 0. \tag{42}$$

So we have

$$\begin{cases} \cos\omega_k - \left(a\alpha\tau h(1 - \frac{2bu_*^2}{d^2}) + h(1-\alpha)\tau\right)\cos m\omega_k = 1 - a\alpha\tau h, \\ \sin\omega_k + \left(a\alpha\tau h(1 - \frac{2bu_*^2}{d^2}) + h(1-\alpha)\tau\right)\sin m\omega_k = 0. \end{cases} \tag{43}$$

Since τ is real and ± 1 are not the roots of Eq. (37), then we get

$$\cos\omega_k = 1 + \frac{h^2\tau^2\left(a\alpha + a\alpha(1 - \frac{2bu_*^2}{d^2}) + (1-\alpha)\right)\left(a\alpha - a\alpha(1 - \frac{2bu_*^2}{d^2}) - (1-\alpha)\right)}{2(1 - a\alpha\tau h)}. \tag{44}$$

If (30) holds, then $\cos\omega > 1$, which leads to conflict. Therefore, Eq. (37) has no root with modulus one for all $\tau > 0$ and sufficiently small $h > 0$. The proof is finished. □

If (24) holds, then $|\cos\omega| < 1$, from (43) and (44) we obtain

$$\omega_k = \arccos\left(\frac{1-\left(a\alpha\tau h(1-\frac{2bu_*^2}{d^2})+h(1-\alpha)\tau\right)^2+(1-a\alpha\tau h)^2}{2(1-a\alpha\tau h)}\right)+2k\pi \tag{45}$$

and

$$\tau_k = \frac{-\sin\omega_k}{\left(a\alpha h(1-\frac{2bu_*^2}{d^2})+h(1-\alpha)\right)\sin m\omega_k}, k=0,1,2,\cdots,\left[\frac{m-1}{2}\right], \tag{46}$$

where $[.]$ represents the greatest integer function. Obviously, there exists a sequence of the τ_k satisfying (43). So we have the following lemma.

Lemma 5. *Suppose $\lambda_k(\tau) = r_k(\tau)e^{i\omega_k(\tau)}$ be a root of characteristic equation Eq. (37), and $r_k(\tau_k) = 1$, $\omega_k(\tau_k) = \omega_k$, if (24) holds, then for any sufficiently small $h > 0$*

$$\frac{dr_k^2(\tau)}{d\tau}|_{\tau=\tau_k,\omega=\omega_k} > 0. \tag{47}$$

Proof. From Eq. (37) we have

$$\lambda^m = \frac{a\alpha\tau h(1-\frac{2bu^2}{d^2})+h(1-\alpha)\tau}{\lambda-1+a\alpha\tau h}, \tag{48}$$

so

$$\bar{\lambda}\frac{d\lambda}{d\tau} = -\frac{\lambda-1}{(a\alpha hm\tau+\lambda(m+1)-m)\tau}, \tag{49}$$

hence, together with (46) we obtain

$$\begin{aligned}\frac{dr_k^2(\tau)}{d\tau}|_{\tau=\tau_k,\omega=\omega_k} &= \left(\lambda\frac{d\bar{\lambda}}{d\tau}+\bar{\lambda}\frac{d\lambda}{d\tau}\right)|_{\tau=\tau_k,\omega=\omega_k} = 2\,\mathrm{Re}\left(\bar{\lambda}\frac{d\lambda}{d\tau}|_{\tau=\tau_k,\omega=\omega_k}\right)\\ &= 2\,\mathrm{Re}\left(-\frac{\lambda-1}{(a\alpha hm\tau+\lambda(m+1)-m)\tau}\right)\\ &= \frac{2(1-\cos\omega_k)(m(2-a\alpha h\tau_k)+1)}{\tau_k|a\alpha hm\tau-m+(m+1)e^{i\omega_k}|^2} > 0.\end{aligned} \tag{50}$$

The proof is complete. □

Theorem 3. *For Eq. (31), the following statements are true:*

(i) If (30) holds, then $u = u_*$ is asymptotically stable for any $\tau \geq 0$.

(ii) If (24) holds, then $u = u_*$ is asymptotically stable for $\tau \in [0, \tau_0)$, and unstable for $\tau > \tau_0$, Eq. (31) undergoes a Hopf bifurcation at u_* when $\tau = \tau_i$, $i = 0, 1, 2, \cdots, [(m-1)/2]$.

Proof. (i) If (30) holds, from Lemmas 3 and 4 we know that Eq. (37) has no root with module one. According to Corollary 2.4 in [11], the conclusion is proved.
(ii) If (24) holds, according to Lemmas 3 and 5 we can get that all roots of Eq. (37) have modules less than one when $\tau \in [0, \tau_0)$, and Eq. (37) has at least a couple of roots with modules greater than one when $\tau > \tau_0$. The conclusion is proved. □

Remark 1. *According to Lemmas 3-5 and Theorem 3, we can delay the onset of the numerical Hopf bifurcation by choosing proper* α.

5. Direction and Stability of the Hopf Bifurcation in Discrete Control System

In this section, we consider the direction and stability of the numerical Hopf bifurcation and the stability of the bifurcating periodic solutions of Eq. (16) when $\tau = \tau_0$ by applying the centre manifold theorem and normal form theory.

Let $\tau = \tau_0 + \mu$, $\mu \in \mathbb{R}$, then $\mu = 0$ is the bifurcation point of the Eq. (16). Expand Eq. (33) at origin gives

$$\begin{aligned} y_{k+1} =& (1 - a\alpha\tau h)y_k + \left(a\alpha\tau h\left(1 - \frac{2bu_*^2}{d^2}\right) + h(1-\alpha)\tau\right) y_{k-m} \\ &+ \frac{a\alpha b\tau h u_*(2bu_*^2 - 3d^2)}{d^4} y_{k-m}^2 + \frac{a\alpha\tau h(12bu_*^2d^2 - 3d^4 - 4b^2u_*^2)}{3d^6} y_{k-m}^3 \\ &+ O(|y_{k-m}|^4). \end{aligned} \tag{51}$$

Then, we can describe Eq. (51) as follows

$$Y_{k+1} = AY_k + \frac{1}{2}B(Y_k, Y_k) + \frac{1}{6}C(Y_k, Y_k, Y_k) + O(\|Y_k\|^4), \tag{52}$$

where

$$B(Y_k, Y_k) = (b_0(Y_k, Y_k), 0, \cdots, 0)^T, C(Y_k, Y_k, Y_k) = (c_0(Y_k, Y_k, Y_k), 0, \cdots, 0)^T,$$

in which

$$\begin{cases} b_0(\phi, \psi) = \tilde{b}\phi_m\psi_m, \\ c_0(\phi, \psi, \eta) = \tilde{c}\phi_m\psi_m\eta_m, \end{cases} \tag{53}$$

here

$$\tilde{b} = \frac{2a\alpha b\tau h u_*(2bu_*^2 - 3d^2)}{d^4}, \tilde{c} = \frac{2a\alpha\tau h(12bu_*^2d^2 - 3d^4 - 4b^2u_*^2)}{d^6}. \tag{54}$$

Let $q = q(\tau_0) \in C^{m+1}$ is the eigenvector corresponding to eigenvalue $e^{i\omega_0}$ and $q^* = q^*(\tau_0) \in C^{m+1}$ is an adjoint vector of q, satisfied $< q^*, q >= 1$, where

$$q = (1, e^{-i\omega_0}, \cdots, e^{-im\omega_0})^T. \tag{55}$$

Lemma 6. *If $\tau = \tau_0$, $q^* = (q_0^*, q_1^*, \cdots, q_m^*)^T$ is the eigenvector of A^T corresponding to eigenvalue $e^{-i\omega_0}$, and $< q*, q >= 1$, then*

$$q^* = \bar{K}(1, a_0 e^{im\omega_0}, a_0 e^{im\omega_0}, \cdots, a_0 e^{i2\omega_0}, a_0 e^{i\omega_0})^T, \tag{56}$$

where $K = 1/(1 + m a_0 e^{-i(m+1)\omega_0})$.

Proof. Let $\bar{z} = e^{-i\omega_0}$. Suppose that $q^* = (q_0^*, q_1^*, \cdots, q_m^*)^T$ is eigenvector corresponding to eigenvalue $\bar{z}$ of A^T, satisfies

$$A^T q^* = \bar{z} q^*. \tag{57}$$

From Eq. (57) we have

$$\begin{cases} a_m q_0^* + q_1^* = e^{-i\omega_0} q_0^*, \\ q_k^* = e^{-i\omega_0} q_{k-1}^*, \quad k = 2, 3, \cdots, m, \\ a_0 q_0^* = e^{-i\omega_0} q_m^*. \end{cases} \tag{58}$$

Let $q_m^* = e^{-i\omega_0}\bar{K}$, then we obtain

$$q^* = \bar{K}(1, a_0 e^{im\omega_0}, a_0 e^{im\omega_0}, \cdots, a_0 e^{i2\omega_0}, a_0 e^{i\omega_0})^T,$$

in view of $< q^*, q >= 1$, the proof is finished. □

Suppose that $a(\lambda)$ is the characteristic polynomial of matrix A, $\lambda_0 = e^{i\omega_0}$. Using the algorithms and the computing method similar to [19], we obtain

$$c_1(\tau_0) = \frac{g_{20} g_{11}(1 - 2\lambda_0)}{2(\lambda_0^2 - \lambda_0)} + \frac{|g_{11}|^2}{1 - \bar{\lambda_0}} + \frac{|g_{02}|^2}{2(\lambda_0^2 - \bar{\lambda_0})} + \frac{g_{21}}{2}, \tag{59}$$

where

$$g_{20} = \langle q^*, B(q, q) \rangle,$$

$$g_{11} = \langle q^*, B(q, \bar{q}) \rangle,$$

$$g_{02} = \langle q^*, B(\bar{q}, \bar{q}) \rangle,$$

$$g_{21} = \langle q^*, B(\bar{q}, \omega_{20}) \rangle + 2 \langle q^*, B(q, \omega_{11}) \rangle + \langle q^*, C(q, q, \bar{q}) \rangle,$$

in which

$$\omega_{20} = \frac{b_0(q, q)}{a(\lambda_0^2)} p(\lambda_0^2) - \frac{\langle q^*, B(q, q) \rangle}{\lambda_0^2 - \lambda_0} q - \frac{\langle \bar{q^*}, B(q, q) \rangle}{\lambda_0^2 - \lambda_0} \bar{q},$$

$$\omega_{11} = \frac{b_0(q,\bar{q})}{a(1)}p(1) - \frac{\langle q^*, B(q,\bar{q})\rangle}{1-\lambda_0}q - \frac{\langle \bar{q}^*, B(q,q)\rangle}{1-\lambda_0}\bar{q}.$$

From (53), (55) and Lemma 6 we calculate that

$$\begin{cases} b_0(\bar{q}, q(e^{i2\omega_0})) = \tilde{b}e^{-im\omega_0}, \\ b_0(q,q) = \tilde{b}e^{-im\omega_0}, \\ b_0(q,\bar{q}) = \tilde{b}, \\ c_0(q,q,\bar{q}) = \tilde{c}e^{-im\omega_0}, \\ a(e^{i2\omega_0}) = e^{i2(m+1)\omega_0} - a_m e^{i2m\omega_0} - a_0, \\ a(1) = 1 - a_m - a_0, \\ b_0(q, q(1)) = \tilde{b}e^{-im\omega_0}. \end{cases} \tag{60}$$

Substituting (60) into (59), we obtain

$$\begin{aligned} c_1(\tau_0) &= \frac{\bar{K}}{2}\left(\frac{\tilde{b}^2}{a(e^{i2\omega_0})} + \frac{2\tilde{b}^2}{a(1)} + \tilde{c}\right) \\ &= \frac{1}{2(e^{im\omega_0} + ma_0e^{-i\omega_0})}\left(\frac{\tilde{b}^2}{e^{i2(m+1)\omega_0} - a_m e^{i2m\omega_0} - a_0} + \frac{2\tilde{b}^2}{1-a_m-a_0} + \tilde{c}\right), \end{aligned} \tag{61}$$

where $\tilde{b}$, $\tilde{c}$ are defined in (54).

Theorem 4. *For Eq. (31), if (24) holds, then $u = u_*$ is asymptotically stable for $\tau \in [0, \tau_0)$, unstable for $\tau > \tau_0$. An attracting (repelling) invariant closed curve exists for $\tau > \tau_0$ if* $\mathrm{Re}[e^{-i\omega_0}c_1(\tau_0)] < 0$ (> 0).

6. Numerical Experiments

In this section, the results in the previous sections are illustrated by some numerical examples. We shall conduct this process from two aspects: controlled system and uncontrolled system. Let $a = 0.2, b = 1, d = 1$, the initial value $u(t) = 1.2$ for $-\tau \le t \le 0$, then $u_* \approx 1.2686$ and $bu_*^2 > d^2$ holds. At the same time, it is easy to compute that (30) holds for $0.6084 < \alpha < 0.8040$ and (24) holds for $\alpha > 0.8040$.

Firstly, we show the graphs of the analytic solution and the numerical solution of Eq. (2) with different τ and $h = 1/100$ in Fig. 1. From this figure we can see that the Euler method has done well in describing the dynamics of the system approximately. For different step sizes and α, we compute the bifurcation points and the direction of bifurcation at equilibrium point in TABLE 1 and TABLE 2, respectively. When $\alpha = 1$, we get the corresponding results for the uncontrolled discrete system naturally. From Theorem 1 and TABLE 1, we conclude that the

equilibrium u_* of Eq. (5) is asymptotically stable for $\tau \in [0, 4.1154)$, unstable for $\tau > 4.1154$. So Eq. (5) undergoes a Hopf bifurcation at u_*. This is what we can see from Figs. 2 and 3.

Next, we show the influence of the hybrid control method on the stability and bifurcation of the system. Specifically, we select different $\alpha \in (0.6084, 0.8040)$ in Fig. 4 and $\alpha = 1 \in (0.8040, 1]$ in Fig. 5, the analytic solution and the phase diagrams of Eq. (16) are displayed in the two figures, respectively. From Theorem 2 we know that the equilibrium point u_* is asymptotically stable for any τ if (30) holds. Moreover, the equilibrium point u_* is asymptotically stable for $\tau \in [0, \tau_0)$, unstable for $\tau > \tau_0$ if (24) holds, where $\tau_0 \approx 4.1154$ which can be obtained from (25), and Eq. (16) undergoes a Hopf bifurcation at u_*. Thus, the phenomenon in Figs. 4-5 are consistent with Theorem 2.

Furthermore, we plot the curves of numerical solution of Eq. (16) and phase diagram of Eq. (31) with $h = 1/10$ and different α (see Figs. 6-11). In view of Theorems 3-4 and TABLE 1, we obtain that the numerical solution is asymptotically stable for $\tau \in [0, \tau_0)$, unstable for $\tau > \tau_0$ and Eq. (31) undergoes a Hopf bifurcation at u_*. This is just what we can see from Figs. 6 and 8. Specifically, in Fig. 6, let $\alpha = 0.9, h = 1/10, \tau = 6$ and 10, respectively. It is easy to observe that the change of numerical solutions from stable to unstable is consistent with Theorems 3-4. We can verify Fig. 8 in the similar way. Moreover, in view of Theorems 3-4 and Table 2, we also obtain that the equilibrium point u_* is asymptotically stable for $\tau \in [0, \tau_0)$, unstable for $\tau > \tau_0$ and Eq. (31) undergoes a Hopf bifurcation at u_*. At the same time, an attracting invariant closed curve exists for $\tau > \tau_0$ and $\mathrm{Re}[e^{-i\omega_0} c_1(\tau_0)] < 0$. This is just what we can see from Figs. 7, 9, 10, 11. More specifically, in Fig. 7, set $\alpha = 0.9, h = 1/10, \tau = 6$ and 10, respectively. We can easily see from this figure that u_* is asymptotically stable for $\tau = 6$ and an attracting invariant closed curve exists for $\tau = 10$. That is, the bifurcation occurs when $\tau > \tau_0 = 6.6824$ and bifurcating periodic solutions from the equilibrium point are orbitally asymptotically stable, which is consistent with Theorems 3-4. We can test the other three figures in a similar fashion.

Furthermore, from the viewpoint of control, we can delay the onset of Hopf bifurcation to improve the stability and enlarge the stability region by choosing appropriate control parameter.

TABLE 1. The values of τ_0 of Hybrid control Euler method

	$\alpha = 1$	$\alpha = 0.9$	$\alpha = 0.85$
h=1/10	4.1154	6.6824	10.3069
h=1/100	5.01203	8.9045	15.2117

TABLE 2. The directions of bifurcation for different α

h=1/10	$c_1(\tau_0)$	$\mathrm{Re}[e^{-i\omega_0}c_1(\tau_0)]$
$\alpha = 1$	-6.1642+1.4390i	-5.8309
$\alpha = 0.9$	-6.2970+1.6429i	-5.9264
$\alpha = 0.85$	-6.3494+1.7819i	-5.9527

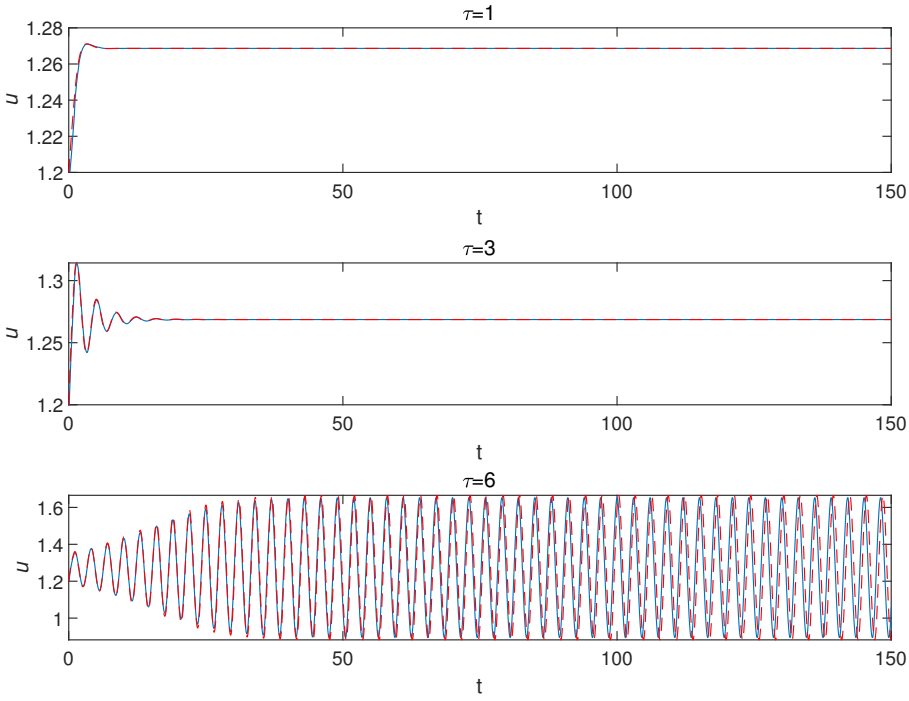

FIGURE 1. The analytic solution (blue solid line) and the numerical solution (red dotted line) of Eq. (2) with $h = 1/100$.

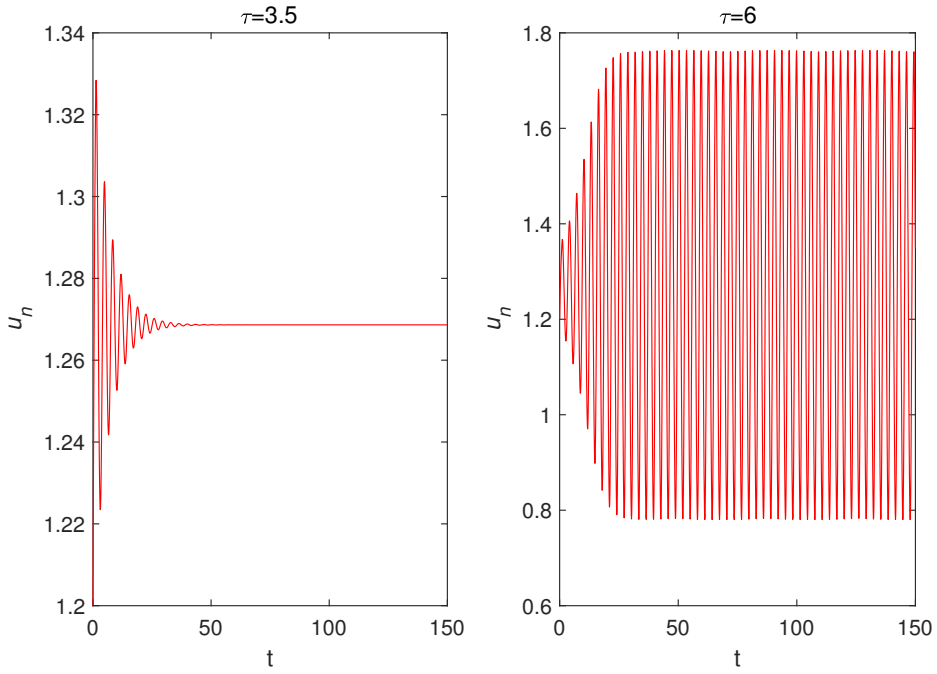

FIGURE 2. The numerical solution of Eq. (16) with $\alpha = 1$, $h = 1/10$ and different τ.

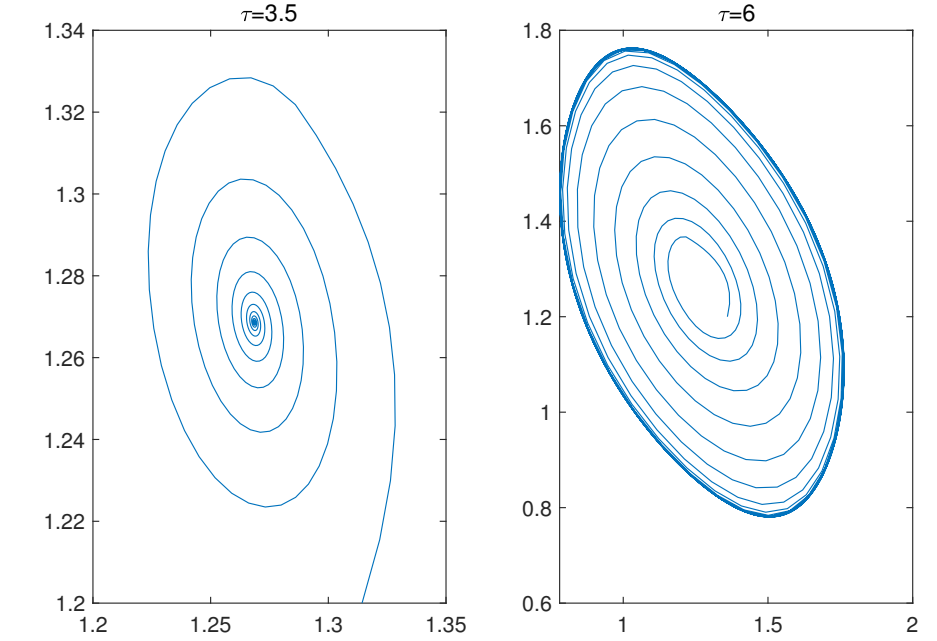

FIGURE 3. The phase diagram of Eq. (31) with $\alpha = 1$, $h = 1/10$ and different τ.

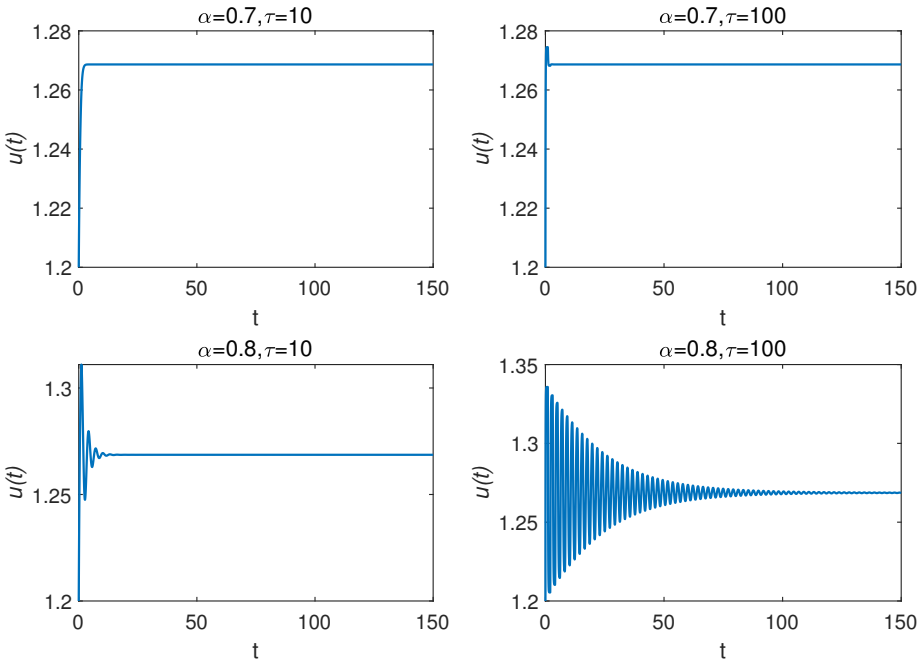

FIGURE 4. The analytic solution of Eq. (16).

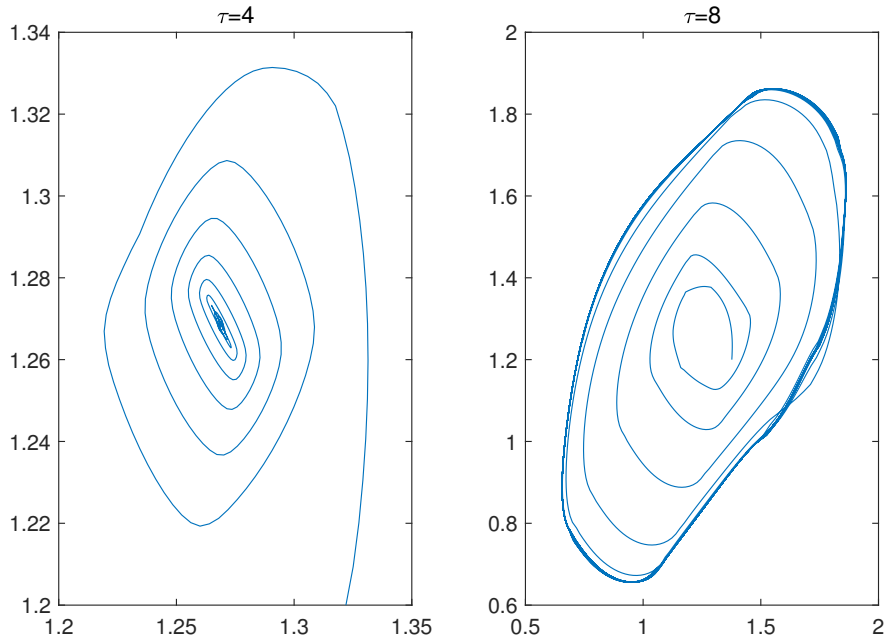

FIGURE 5. The phase diagram of Eq. (16) with $\alpha = 1$.

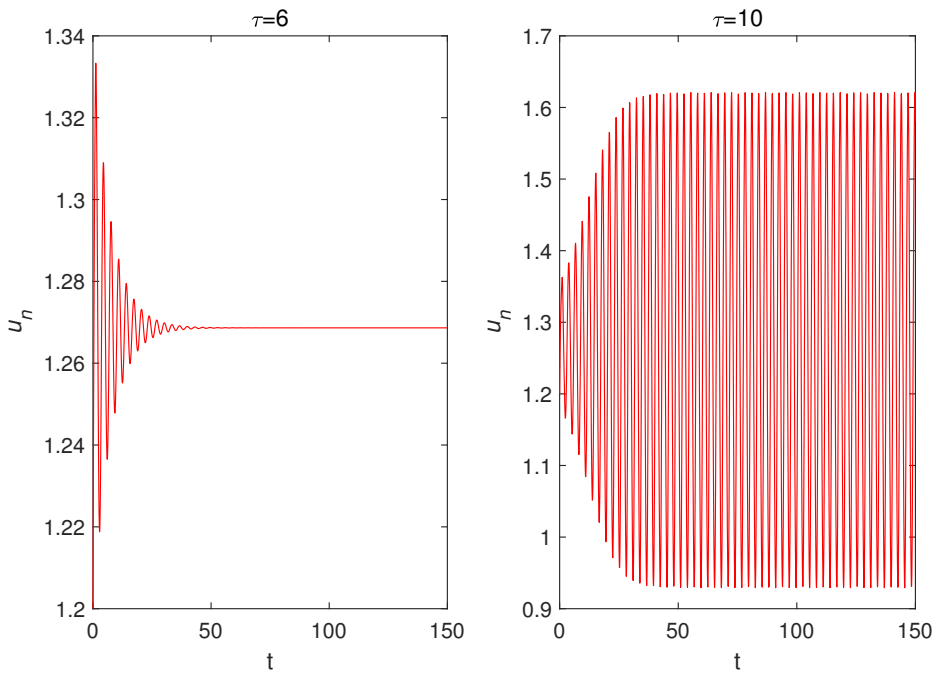

FIGURE 6. The numerical solution of Eq. (16) with $\alpha = 0.9$ and $h = 1/10$.

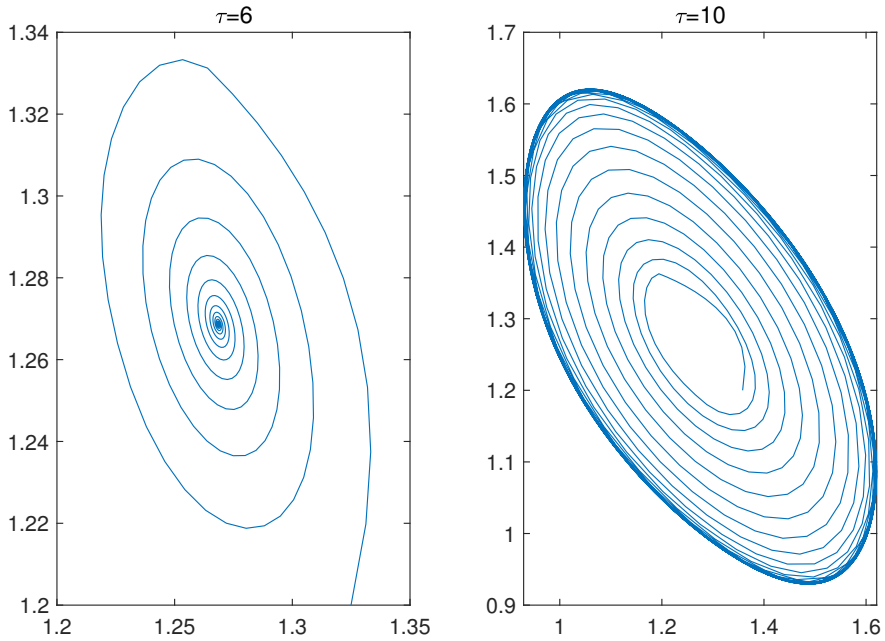

FIGURE 7. The numerical phase diagram of Eq. (31) $h = 1/10$ and $\alpha = 0.9$.

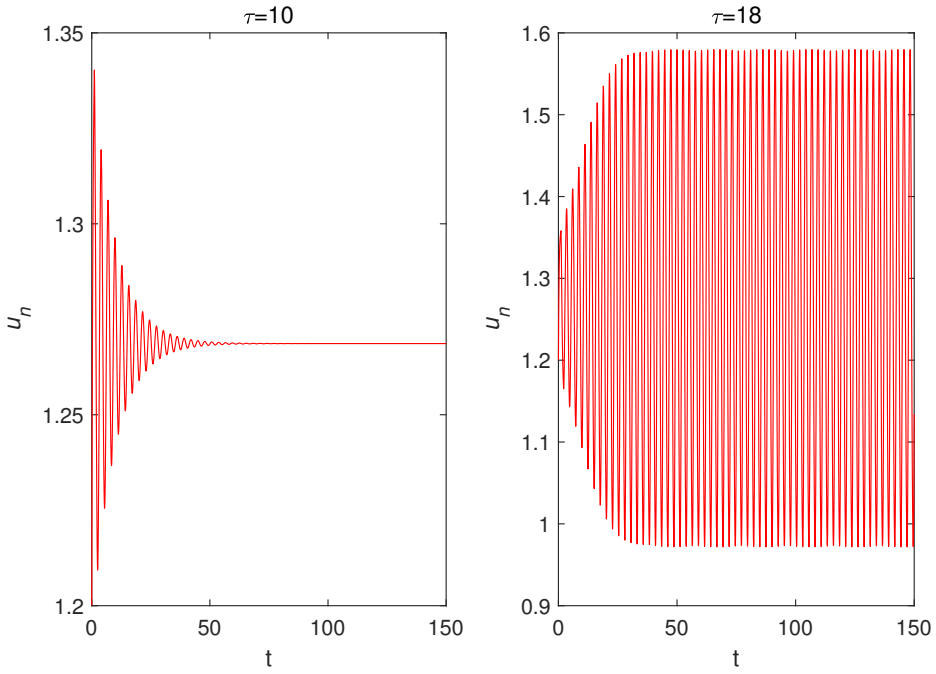

FIGURE 8. The numerical solution of Eq. (16) with $\alpha = 0.85$ and $h = 1/10$.

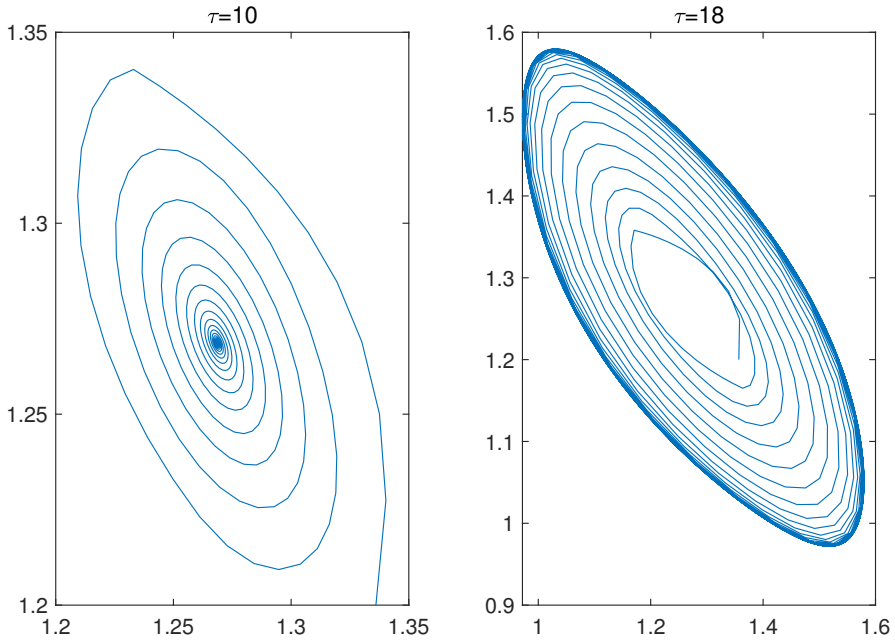

FIGURE 9. The numerical phase diagram of Eq. (31) with $h = 1/10$ and $\alpha = 0.85$.

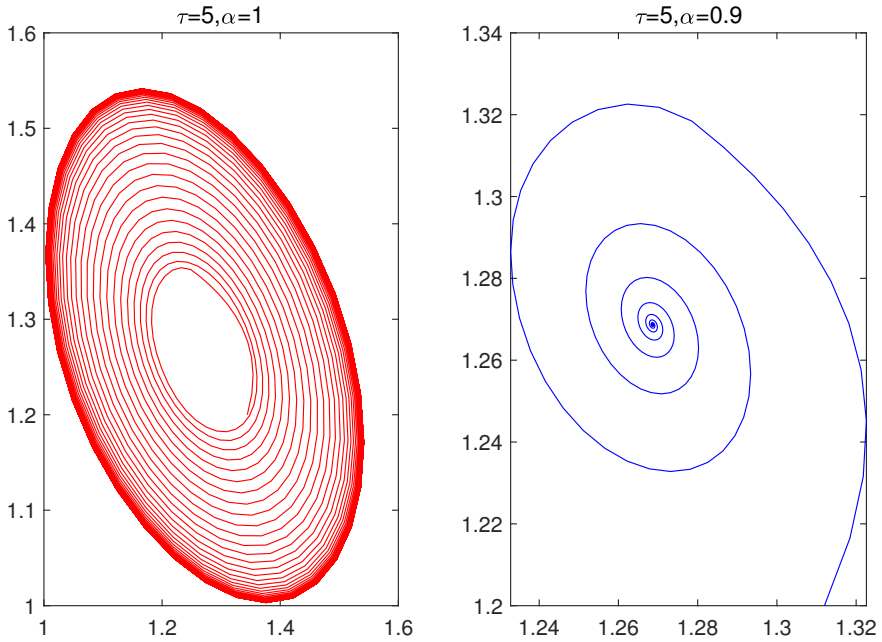

FIGURE 10. The numerical phase diagram of Eq. (31) with $\tau = 5$ and $h = 1/10$ for different α.

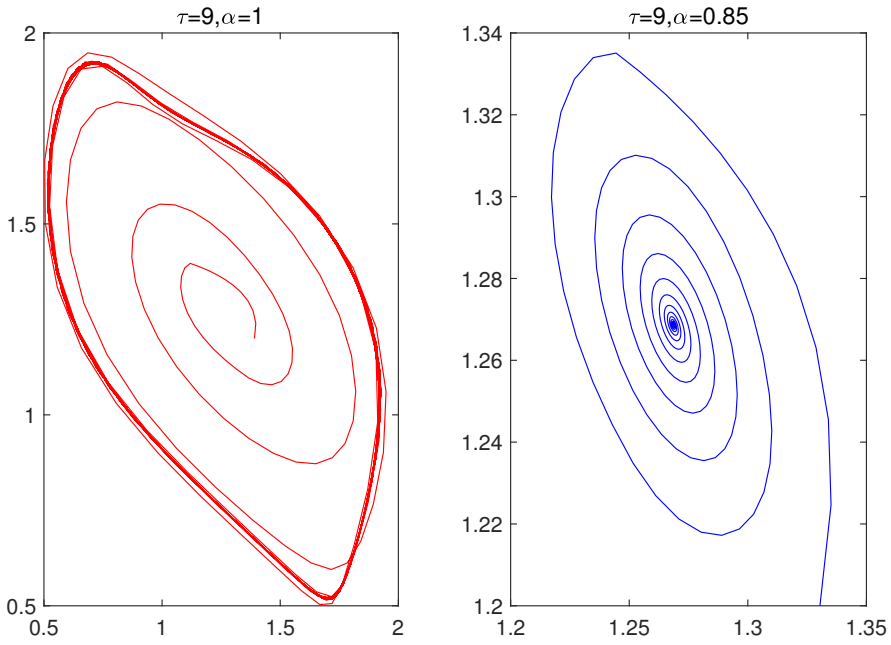

FIGURE 11. The numerical phase diagram of Eq. (31) with $\tau = 9$ and $h = 1/10$ for different α.

Acknowledgements

This research is supported by the Natural Science Foundation of Guangdong Province (No. 2017A030313031).

Data Availability

The data used to support the findings of this study are available from the corresponding author upon request.

Conflicts of Interest

The authors declare that they have no conflicts of interest.

References

[1] G.I. Bischi, L. Gardini, M. Kopel, Analysis of global bifurcations in a market share attraction model, J. Econ. Dyn. Control. 24 (2000), 855-879. https://doi.org/10.1016/s0165-1889(99)00028-7.

[2] L. Fei, X. Chen, B. Han, Bifurcation analysis and hybrid control of a discrete-time predator-prey model, J. Differ. Equ. Appl. 27 (2021), 102-117. https://doi.org/10.1080/10236198.2021.1876038.

[3] R.S. Gao, J. Ruan, Hopf bifurcation of nonlinear advertising capital model with discrete and continuous time delayed feedback, Ann. Appl. Math. 23 (2007), 264-272.

[4] T.P. Hsieh, C.Y. Dye, K.K. Lai, A dynamic advertising problem when demand is sensitive to the credit period and stock of advertising goodwill, J. Oper. Res. Soc. 71 (2019), 948-966. https://doi.org/10.1080/01605682.2019.1595189.

[5] C. Huang, H. Li, J. Cao, A novel strategy of bifurcation control for a delayed fractional predator-prey model, Appl. Math. Comput. 347 (2019), 808-838. https://doi.org/10.1016/j.amc.2018.11.031.

[6] A.Q. Khan, T. Khalique, Neimark?Sacker bifurcation and hybrid control in a discrete?time Lotka?Volterra model, Math. Methods Appl. Sci. 43 (2020), 5887-5904. https://doi.org/10.1002/mma.6331.

[7] X. Long, S. Gong, New results on stability of Nicholson?s blowflies equation with multiple pairs of time-varying delays, Appl. Math. Lett. 100 (2020), 106027. https://doi.org/10.1016/j.aml.2019.106027.

[8] I. Luhta, I. Virtanen, Non-linear advertising capital model with time delayed feedback between advertising and stock of goodwill, Chaos Solitons Fractals. 7 (1996), 2083-2104. https://doi.org/10.1016/s0960-0779(96)00074-4.

[9] X.Y. Meng, J.G. Wang, Dynamical analysis of a delayed diffusive predator-prey model with schooling behaviour and Allee effect, J. Biol. Dyn. 14 (2020), 826-848. https://doi.org/10.1080/17513758.2020.1850892.

[10] M. Nerlove, K.J. Arrow, Optimal advertising policy under dynamic conditions, Economica. 29 (1962), 129-142. https://doi.org/10.2307/2551549.

[11] S. Ruan, J.J. Wei, On the zeros of transcendental functions with applications to stability of delay differential equations with two delays, Dyn. Contin. Discrete Impulsive Syst. Ser. A: Math. Anal. 10 (2003), 863-874.

[12] H. Shu, W. Xu, X.S. Wang, J. Wu, Complex dynamics in a delay differential equation with two delays in tick growth with diapause, J. Differ. Equ. 269 (2020), 10937-10963. https://doi.org/10.1016/j.jde.2020.07.029.

[13] Q. Wang, J. Wen, P. Zhang, Oscillation analysis of advertising capital model: Analytical and numerical studies, Appl. Math. Comput. 354 (2019), 365-376. https://doi.org/10.1016/j.amc.2019.02.029.

[14] Z. Wang, L. Li, Y. Li, Z. Cheng, Stability and hopf bifurcation of a three-neuron network with multiple discrete and distributed delays, Neural Process Lett. 48 (2018), 1481-1502. https://doi.org/10.1007/s11063-017-9754-8.

[15] Y. Wang, PD control at Neimark-Sacker bifurcations in a Mackey-Glass system, Adv. Differ. Equ. 2018 (2018), 411. https://doi.org/10.1186/s13662-018-1864-8.

[16] Y. Wang, L. Wang, Hybrid control of the Neimark-Sacker bifurcation in a delayed Nicholson?s blowflies equation, Adv. Differ. Equ. 2015 (2015), 306. https://doi.org/10.1186/s13662-015-0640-2.

[17] Z. Wei, Q. Yang, Anti-control of Hopf bifurcation in the new chaotic system with two stable node-foci, Appl. Math. Comput. 217 (2010), 422-429. https://doi.org/10.1016/j.amc.2010.05.035.

[18] V. Wulf, N.J. Ford, Numerical Hopf bifurcation for a class of delay differential equations, J. Comput. Appl. Math. 115 (2000), 601-616. https://doi.org/10.1016/s0377-0427(99)00181-8.

[19] V. Wulf, Numercial analysis of delay differential equations undergoing a Hopf bifurcation, University of Liverpool, Liverpool, (1999).

[20] X.S. Luo, G. Chen, B. Hong Wang, J. Qing Fang, Hybrid control of period-doubling bifurcation and chaos in discrete nonlinear dynamical systems, Chaos Solitons Fractals. 18 (2003), 775-783. https://doi.org/10.1016/s0960-0779(03)00028-6.

[21] C. Xu, Q. Li, T. Zhang, S. Yuan, Stability and Hopf bifurcation for a delayed diffusive competition model with saturation effect, Math. Biosci. Eng. 17 (2020), 8037-8051. https://doi.org/10.3934/mbe.2020407.

[22] P. Yu, J. Lu, Bifurcation control for a class of Lorenz-like systems, Int. J. Bifurcation Chaos. 21 (2011), 2647-2664. https://doi.org/10.1142/s0218127411030003.

[23] C. Zhang, Y. Zu, B. Zheng, Stability and bifurcation of a discrete red blood cell survival model, Chaos Solitons Fractals. 28 (2006), 386-394. https://doi.org/10.1016/j.chaos.2005.05.042.